Available online at www.sciencedirect.com
ScienceDirect
Toxicology in Vitro 22 (2008) 308–317
Toxicology in Vitro
www.elsevier.com/locate/toxinvit

Effect of chlorhexidine digluconate on different cell types: A molecular and ultrastructural investigation

M. Giannelli [a,*], F. Chellini [b], M. Margheri [b], P. Tonelli [a], A. Tani [b,*]

[a] Department of Oral Surgery, University of Florence, Viale Morgagni 85, 50134 Florence, Italy
[b] Department of Anatomy, Histology and Forensic Medicine, University of Florence, Viale Morgagni 85, 50134 Florence, Italy

Received 18 July 2007; accepted 14 September 2007
Available online 5 November 2007

Abstract

Although several studies have shown that chlorhexidine digluconate (CHX) has bactericidal activity against periodontal pathogens and exerts toxic effects on periodontal tissues, few have been directed to evaluate the mechanisms underlying its adverse effects on these tissues. Therefore, the aim of the present study was to investigate the *in vitro* cytotoxicity of CHX on cells that could represent common targets for its action in the surgical procedures for the treatment of periodontitis and peri-implantitis and to elucidate its mechanisms of action.

Osteoblastic, endothelial and fibroblastic cell lines were exposed to various concentrations of CHX for different times and assayed for cell viability and cell death. Also analysis of mitochondrial membrane potential, intracellular Ca^{2+} mobilization and reactive oxygen species (ROS) generation were done in parallel, to correlate CHX-induced cell damage with alterations in key parameters of cell homeostasis. CHX affected cell viability in a dose and time-dependent manners, particularly in osteoblasts. Its toxic effect consisted in the induction of apoptotic and autophagic/necrotic cell deaths and involved disturbance of mitochondrial function, intracellular Ca^{2+} increase and oxidative stress.

These data suggest that CHX is highly cytotoxic *in vitro* and invite to a more cautioned use of the antiseptic in the oral surgical procedures.

Keywords: Chlorhexidine; Cell culture; Cell viability; Calcium transients; ROS generation

1. Introduction

It is well documented that chronic periodontitis and peri-implantitis represent the main cause of teeth and implants loss in the adult population. Since the pathogenesis of these diseases is mainly related to multiple infective agents (Slots and Genco, 1984; Mombelli et al., 1987; Becker et al., 1990; Eke et al., 1998; Listgarten and Lai, 1999), several attempts have been developed for the eradication of microorganisms from the root and implant surface with the use of mechanical procedures combined with antimicrobial agents (Cadosch et al., 2003; Vianna et al., 2004). Indeed, owing to the technical difficulties of access to the anatomical structures for instrumentations, the use of conventional mechanical methods alone (i.e.,

Abbreviations: BSA, bovine serum albumin; CHX, Chlorhexidine digluconate; CLSM, confocal laser scanning microscopy; CM-H_2 DCFDA, fluorogenic substrate, 5-(and-6)-chloromethyl-2′,7′-dichlorodihydrofluorescin diacetate, acetyl ester; DCF, 2′,7′-dichlorofluorescein; DMEM, Dulbecco's modified Eagle's medium; FA, focal adhesion; Fluo-3 AM, Fluo-3-acetoxymethyl ester; ISEL, *in situ* end labeling of nicked DNA; JC-1, 5,5′,6,6′-tetrachloro-1,1′,3,3′-tetraethylbenzimidazolyl-carbocyanine iodide; MTS, 3-(4.5-dimethylthiazol-2-yl)-5-(3-carboxymethoxyphenyl)-2-(4-sulfophenyl)-2H-tetrazolium; PBS, phosphate buffered saline; ROS, reactive oxygen species; TEM, transmission electron microscopy; TRITC, tetra methyl rhodamine isothiocyanate.

* Corresponding authors. Tel./fax: +39 055 411798 (M. Giannelli), Tel.: +39 055 410084; fax: +39 055 4379500 (A. Tani).
E-mail addresses: dott.giannellimarco@dada.it (M. Giannelli), alessia.tani@unifi.it (A. Tani).

0887-2333/$ - see front matter © 2007 Elsevier Ltd. All rights reserved.
doi:10.1016/j.tiv.2007.09.012

scaling and root planning) cause only a temporary decrease in the subgingival levels of pathogens and endotoxins (Sbordone et al., 1990; Drisko, 2001; Renvert et al., 2006), without blocking the pathological process (Mombelli and Lang, 1992). Moreover, the complexity of the implant surfaces provided with threads or roughness, make the mechanical management of peri-implant infection almost unfeasible (Mombelli and Lang, 1992). In particular, since intact implant roughness and titanium oxide layer are essential for modulating osteoblasts migration from the implant tissue interface and favouring their attachment and proliferation on the implant surface, decontaminating implants with mechanical devices may seriously affect the surface properties and compromise the possible re-osseointegration of implant (Mustafa et al., 2000; Shibli et al., 2003). In this connection, the chemotherapeutic approaches for treatment of periodontal and peri-implant disease, including topical application of antiseptic agents such as hydrogen peroxide, povidone-iodine (Quirynen et al., 1995; Hoang et al., 2003) or the sustained release of local drugs such as tetracycline, minocycline, doxycycline and metronidazole (Drisko et al., 1995; Stelzel and Flores-de-Jacoby, 1996; Jeffcoat et al., 1998; Buchter et al., 2004; Renvert et al., 2006) has been shown to largely increase the benefits obtained by conventional mechanical treatment. The application of chlorhexidine (CHX) is considered the gold standard antiseptic treatment, since this agent is one of the most extensively used and tested, especially in consideration of its high bactericidal capability, its ability to inhibit glycosydic and proteolytic activities and to reduce matrix metalloproteinases activities in a huge variety of oral bacteria (Beighton et al., 1991; Gendron et al., 1999; Cronan et al., 2006) and its efficacy in the treatment of oral infections (Quirynen et al., 1995; Pitten and Kramer, 1999). However, evidences are emerging suggesting that this compound may also have adverse effects on oral tissues and cells at the concentrations used clinically. Indeed, several studies have reported that CHX: (i) has cytotoxic activity on cultured alveolar bone (Cabral and Fernandes, 2007) and gingival epithelial cells (Babich et al., 1995); (ii) induces a dose-dependent reduction of human gingival fibroblast proliferation and reduces both collagen and non-collagen protein production at concentrations with little effect on cellular proliferation (Pucher and Daniel, 1992; Cline and Layman, 1992; Mariotti and Rumpf, 1999); (iii) prevents fibroblast attachment to root surfaces and interferes with periodontal regeneration (Alleyn et al., 1991); (iv) is able to induce primary DNA damage in leukocytes and oral mucosal cells of rats treated daily with the compound (Ribeiro et al., 2004) and; (v) exerts genotoxic side effects on epithelial and blood cells when used for mouth rinsing in clinical trials (Eren et al., 2002). To further complicate this scenario and hamper the efficacy of the CHX treatment in the dental practice, there are data showing that only very high concentrations of CHX (0.5–2% for 10 min) can achieve substantial bactericidal effect against periodontal pathogens (Oosterwaal et al., 1989). Moreover, some periodontal microorganisms have been shown to be only moderately susceptible to this compound (Slots et al., 1991; Rams and Slots, 1996).

On the basis of these observations and in consideration of the widespread use of CHX for topical oral surgical preparation and for the treatment of periodontal and peri-implant diseases, the current study was designed to examine the effects of CHX on cell viability and cell death in different cell types (fibroblasts, endothelial and osteoblastic cells) that could represent common targets for the toxic substance in the oral surgical procedure. We also aimed to investigate the mechanisms underlying the potential cytotoxicity of the antiseptic on these cells.

2. Materials and methods

2.1. Cell culture and treatment

Osteoblastic Saos-2, from human osteosarcoma cells, obtained from American Type Culture Collection (ATCC) (Manassas, VA, USA), were cultured in F12-Coon's modification medium (Sigma, St. Louis, MO, USA) containing 10% fetal bovine serum (Sigma), 100 U/ml penicillin–streptomycin. Murine fibroblasts NIH/3T3 cells obtained from ATCC and murine endothelioma H-end cells obtained from Cambrex (Walkersville, MD, USA) were cultured in Dulbecco's modified Eagle's medium (DMEM) (Sigma) with 4.5 g/l glucose, supplemented with 10% bovine calf serum (HyClone, Perbio Company, Logan, UT, USA) and fetal calf serum (Sigma) respectively, penicillin (100 U/ml) and streptomycin (100 μg/ml) (Sigma). The cells were grown at 37 °C in a humidified atmosphere of 5% CO_2, then treated with different concentrations (0.0025%, 0.005%, 0.0075%, 0.01% and 0.12%) of chlorhexidine digluconate (Sigma) for different times (1 min, 5 min and 15 min), and finally shifted in complete fresh medium for further 4 h.

2.2. Cell viability assay (MTS)

Cell viability was determined by 3-(4.5-dimethylthiazol-2-yl)-5-(3-carboxymethoxyphenyl)-2-(4-sulfophenyl)-2H-tetrazolium (MTS) assay (Promega Corp., Madison, WI, USA), a colorimetric method for determining the number of viable cells in cytotoxicity assays. The dye is reduced by the mitochondrial enzyme succinate dehydrogenase to produce a colored formazan product in live cells, as previously described (Mosmann, 1983). To this purpose, the cells were plated in 96-well plates (1.5×10^4 cells/well) and, after 48 h of incubation, were treated with CHX in phenol red-free medium for 1, 5 and 15 min. Then the cells were shifted in 100 μl of fresh medium and 20 μl of MTS test solution was added to each well. After 4 h of incubation, the optical density (OD) of soluble formazan was measured using a multi-well scanning spectrophotometer (ELISA reader) (Amersham, Pharmacia Biotech, Cambridge, UK) at a wavelength of 490 nm. The values are

expressed as mean ± SD obtained from five independent experiments carried out in triplicates.

2.3. Confocal immunofluorescence

Cells grown for 48 h on glass coverslips both untreated and treated with CHX for the different times, were fixed in 0.5% buffered paraformaldehyde for 10 min at room temperature. After permeabilization with cold acetone for 3 min, the fixed cells were blocked with 0.5% bovine serum albumin (BSA) (Sigma) and 3% glycerol in PBS for 20 min and then incubated with primary antibody monoclonal anti-vinculin (1:100, Sigma) for 1 h at room temperature. After washing, the cells were further incubated for 1 h at room temperature with Alexa 488 IgG (1:100, Molecular Probes, Eugene, OR, USA), rinsed and mounted with an antifade mounting medium (Biomeda Gel mount, Electron Microscopy Sciences, Foster City, CA, USA). Negative control was carried out by replacing the primary antibody with non-immune mouse serum. Counterstaining was performed with tetra methyl rhodamine isothiocyanate (TRITC)-labeled phalloidin (1:100, Sigma) for 1 h at room temperature to reveal F-actin organization. Cells were then examined with a Bio-Rad MCR 1024 ES Confocal Laser Scanning Microscope (CLSM) (Bio-Rad, Hampstead, UK) equipped with a Krypton/Argon (Kr/Ar) laser source (15 mW) for fluorescence measurements and with differential interference contrast optics. Fluorescence was collected by a Nikon Plan Apo X 60 oil immersion objective (Melville, NY, USA). Series of optical sections (512 × 512 pixels) at intervals of 0.4 μm were taken and superimposed as a single composite image. The laser potency, photomultiplier and pin-hole size were kept constant.

2.4. Evaluation of apoptosis by ISEL assay

In situ end labeling of nicked DNA (ISEL assay) was performed on untreated and treated cells, according to the manufacturer's instructions. Briefly, after a treatment with 20 μg/ml of proteinase K to remove the excess protein from nuclei, and inactivation of endogenous peroxidases with H_2O_2, the cells were incubated with the Klenow fragment of DNA polymerase I and biotinylated deoxynucleotides (FRAGEL-Klenow, DNA fragmentation kit, Calbiochem, San Diego, CA, USA) in a humidified chamber at 37 °C for 1.5 h. After that, the cells were incubated with streptoavidin-peroxidase for 10 min and stained with diaminobenzidine tetrahydrochloride (DAB). Counterstaining was performed with methyl green. Quantification of ISEL-positive cells was performed by examining at least five different optical fields of 138,000 μm^2 at 540× magnification in each sample. In each field, which contained ~80 cells, the number of positive cells was recorded and the percentage of these cells over the total cells was calculated. Two different observers evaluated the same microscopic fields and individual values were then averaged.

2.5. Assessment of mitochondrial membrane potential

The alteration of mitochondrial membrane potential in untreated and treated cells (osteoblastic, endothelial and fibroblastic cells) was determined by 5,5′,6,6′-tetrachloro-1,1′,3,3′-tetraethylbenzimidazolyl-carbocyanine iodide (JC-1) (Molecular Probes) assay. Untreated and treated cells grown on glass coverslips were incubated with 1 ml of DMEM w/o phenol red containing 2 μg/ml of JC-1 for 15 min at 37 °C. Subsequently, the specimens were rinsed with PBS, mounted in open-slide flow-loading chamber and placed onto the stage of a confocal microscope. Fluorescence images were collected by a Nikon Plan Apo × 60 oil immersion objective using 488/564 nm excitation wavelengths. JC-1 is a cationic dye whose emitted fluorescence changes from red (J-aggregates) to green (JC-1 monomers) following a mitochondrial membrane depolarization. In each experimental condition, the ratio of red/green fluorescent signal was calculated in 80 randomly selected cells by measuring the average intensities of the emitted fluorescence using Image J (NIH) software.

2.6. Ultrastructural analysis

For transmission electron microscopy (TEM) analysis, the cells were cultured in flasks to obtain a confluence of 90%, treated with CHX (0.01%) for 1 min, and shifted in fresh medium for 2 h. The cells, untreated and treated, were then rinsed, detached and, after centrifugation, the pellets were immediately fixed in 4% cold glutaraldehyde in 0.2 M sodium cacodylate buffer, pH 7.4, for 1 h at room temperature, and postfixed in 1% osmium tetroxide in 0.1 M phosphate buffer, pH 7.4, for 1 h at 4 °C. The pellets were then dehydrated in graded acetone, passed through propylene oxide and embedded in Epon 812. Semi-thin sections, 2 μm thick, were cut, stained with toluidine blue sodium tetraborate and observed under light microscope. Ultrathin sections were also obtained from the same specimens stained with uranyl acetate and alkaline bismute subnitrate and then examined under transmission electron microscopy at 80 kV. For a quantitative evaluation of cell death, a mean of 1500 cells were scored for ultrathin sections. The number of dead cells (i.e. cells showing disrupted plasma membrane, pyknotic nuclei, cytoplasmic swelling and/or apoptotic nuclear fragmentation) was expressed as the percentage of the total cells.

2.7. Confocal analysis of calcium transients

To reveal variations in intracellular concentrations of calcium, the cells were plated on glass coverslips and incubated at room temperature for 10 min in serum-free DMEM with 0.1% BSA containing Fluo-3-acetoxymethyl ester (1 μM), as fluorescent Ca^{2+} dye, 0.1% anhydrous dimethyl sulfoxide and Pluronic F-127 (0.01% wt/vol) as dispersing agent (Molecular Probes). The cells were then washed and maintained in fresh medium for 10 min to

allow the complete de-esterification of Fluo 3-AM. After that, the cells were placed in open-slide flow-loading chambers and mounted on the stage of a confocal microscope. CHX (0.01% for the osteoblastic cells and 0.12% for fibroblasts and endothelial cells) or vehicle was added to loaded cells and Fluo 3-AM fluorescence was monitored using a 488 nm wavelength. Fluorescence images were collected with a Nikon Plan Apo ×60 oil immersion objective through a 510 nm long-wave pass filter. The time course analysis of Ca^{2+} transients, after CHX stimulation, was performed using a Time Course Kinetic software (Bio-Rad).

2.8. Analysis of ROS generation

ROS generation was determined using the fluorogenic substrate 5-(and-6)-chloromethyl-2′,7′-dichlorodihydrofluorescin diacetate, acetyl ester (CM-H_2 DCFDA) (Molecular Probes), as previously described (Pieri et al., 2006; Wardman, 2007). Briefly, Saos-2 cells were grown on glass coverslips, treated with 0.01% CHX for 1 min and then loaded with 5 μM CM-H_2 DCFDA for 20 min at 37 °C. After that, the cells were washed with PBS to remove CM-H_2 DCFDA and mounted in open-slide flow-loading chambers on the stage of the confocal microscope. The levels of ROS were visualized by determining the fluorescence intensity of 2′,7′-dichlorofluorescein (DCF) at 488 nm wavelength and using a Time Course Kinetic software.

2.9. Statistical analysis

All data are presented as mean ± standard deviation (SD). Comparisons between the different groups were performed by ANOVA followed by the Bonferroni *t*-test. Values of $P < 0.05$ and $P < 0.01$ were accepted as statistically significant.

3. Results

3.1. Effects of chlorhexidine on cell viability

MTS assay showed that the treatment with CHX affected cell viability in a dose and time-dependent manner (Fig. 1). Saos-2 cells appeared highly sensitive to the treatment, since their viability was significantly reduced (approximately by 57.5%, $P < 0.05$) after exposure to 0.01% concentration of CHX for 1 min. The progressive increase in the concentration of the antiseptic agent (from 0.03% to 0.12%) correlated with a parallel increase in the osteoblastic cell death (up to 80%). By contrast, fibroblastic NIH/3T3 and endothelial H-end cells appeared to be more resistant to the treatment, showing a significant reduction of cell viability (60–80%, $P < 0.05$) upon treatment with higher concentrations (0.03–0.12%) of CHX. Long-term treatments (5, 15 min) induced a massive cell death in all the cell types at any concentration.

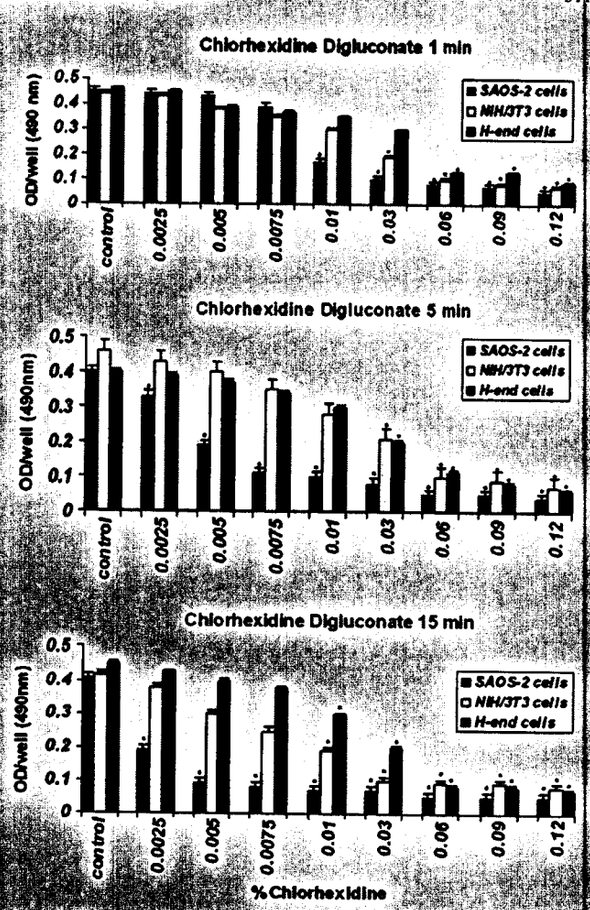

Fig. 1. Effects of CHX on cell viability. Dose and time-dependent response of Saos-2, NIH/3T3 and H-end cells to CHX by MTS assay. The cells were treated at the indicated concentrations of CHX for the indicated time points. The cells were then shifted in complete fresh medium containing 20 μl of MTS test for further 4 h. MTS reduction was measured by a spectrophotometer. The values are expressed as mean ± SD obtained from five independent experiments carried out in triplicates.

At confocal microscopy, the treatment of the osteoblastic Saos-2 cells with 0.01% CHX caused a dramatic alteration in the cytoskeletal organization followed by rounding up of the cells and progressive detachment from the substrate, suggesting the ability of the compound to induce irreversible cell damage. Previous reports have, in fact, shown that actin disarrangement leads to cell growth arrest and apoptosis (Gourlay and Ayscough, 2006; Anuradha et al., 2007). In particular, in untreated Saos-2 cells, actin filaments were arranged in a web-like structure which was anchored to the plasma membrane through focal adhesion (FA) sites containing vinculin (Fig. 2A). After treatment, the filaments appeared dispersed and the FA irregularly distributed within the cytoplasm (Fig. 2B). Fibroblastic and endothelial cell cultures exposed to higher levels (0.12%) of CHX presented a similar behavior (data not shown).

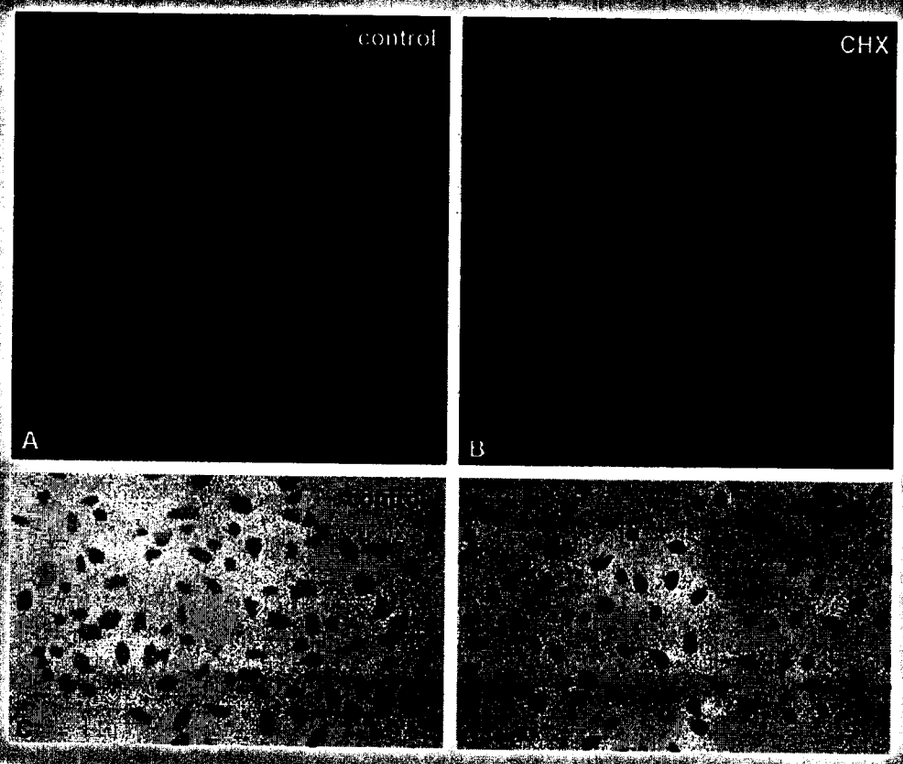

Fig. 2. Effects of CHX on cytoskeletal organization and apoptotic cell death. (A, B) Saos-2 cells untreated (control) and treated with 0.01% CHX for 1 min were fixed and double stained with TRITC-phalloidin (red) to reveal actin filaments and anti-vinculin (green) antibodies to detect FA sites. The untreated cells (A) show a well organized actin cytoskeleton anchored to the plasma membrane through FA sites containing vinculin; by contrast, the treated cells (B) display a loss of actin filaments and a round-shaped morphology (900×). (C, D) Detection of apoptosis by ISEL assay in Saos-2 cells untreated (control) and treated with CHX 0.01% for 1 min. The untreated cells (C) display green nuclei, whereas the treated cells (D) show brown-stained nuclei, indicating the execution of nuclear apoptotic degradation (200×). All the images are representative of at least three independent experiments with similar results.

3.2. Detection of apoptotic and necrotic cell death in chlorhexidine-treated cells

In order to investigate the apoptosis-inducing activity of CHX, the cells were processed for ISEL assay. By this technique, the apoptotic cells may be easily recognized by the presence of a brown nuclear staining indicative of DNA fragmentation, whereas the nucleus of viable cells appears green. After 1 min treatment, more than 30% of Saos-2 cells (exposed to 0.01% CHX) and nearly 50% of fibroblastic and endothelial cells (treated with 0.12% CHX) exhibited apoptotic nuclei (Fig. 2C and D). In the treated osteoblasts, the amount of cells undergoing apoptotic nuclear fragmentation increased upon exposure to higher concentration (0.12%), reaching almost 80% of the total cells.

Transmission electron microscopy revealed that apoptosis was not the only type of cell death induced by the treatment with CHX. Indeed, after treatment with 0.01% CHX for 1 min, osteoblasts showing typical apoptotic signs, including condensed nuclear chromatin, fragmented DNA, extensive cytoplasmic vacuolization and blebbing (Fig. 3A and B), represented approximately 10–15% of the total population and coexisted with cells exhibiting distinct features of necrotic cell death (Fig. 3C). These cells, which accounted for approximately 20% of the total cell population, revealed an intact nucleus with dispersed chromatin cytoplasmic vacuolization, loss of plasma membrane integrity with spillage of the cytoplasmic content nearby. Some of them contained large autophagic vacuoles (Fig. 3D). Quite similar ultrastructural changes were also detected in endothelial cells and NIH/3T3 fibroblasts treated with CHX (data not shown).

3.3. Effects of chlorhexidine on mitochondrial function

With the aim of investigating whether CHX-induced cytotoxicity was associated with mitochondrial dysfunctions, we performed functional studies to investigate the integrity of the mitochondrial membrane potential using the mitochondria specific fluorochrome JC-1. Compared with untreated cells (Fig. 4A), whose cytoplasm was packed with thread-like energized red mitochondria, the osteoblasts exposed to 0.01% CHX for 1 min (Fig. 4B), exhibited green mitochondrial fluorescence, which was consistent with the loss of mitochondrial trans-membrane polarization, a

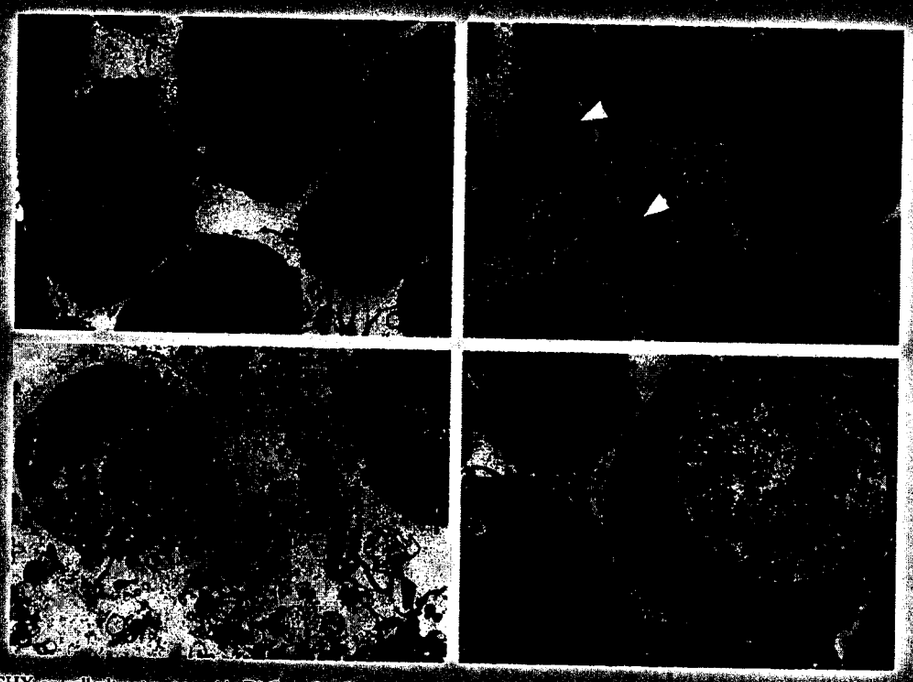

Fig. 3. Effects of CHX on cell ultrastructure. (A–D) Saos-2 cells were treated with 0.01% CHX for 1 min and then shifted in complete fresh medium for further 4 h. After that, the cells were routinely processed for TEM analysis. With respect to the untreated cells (A), the treated ones (B) display apoptotic features (arrows), including nuclear condensed chromatin, cytoplasmic condensation and blebbing. Moreover, some of the treated cells (C, D) show signs of autophagic/necrotic cell death. Note the presence of dissolution of plasma membranes with spillage of the cytoplasmic content in some osteoblasts (C, 4000×) and the presence of a large autophagic vacuole filled with organelles and electron-dense fuzzy materials in other cells (D, arrow) (A, B, C, 4000×; D, 5000×).

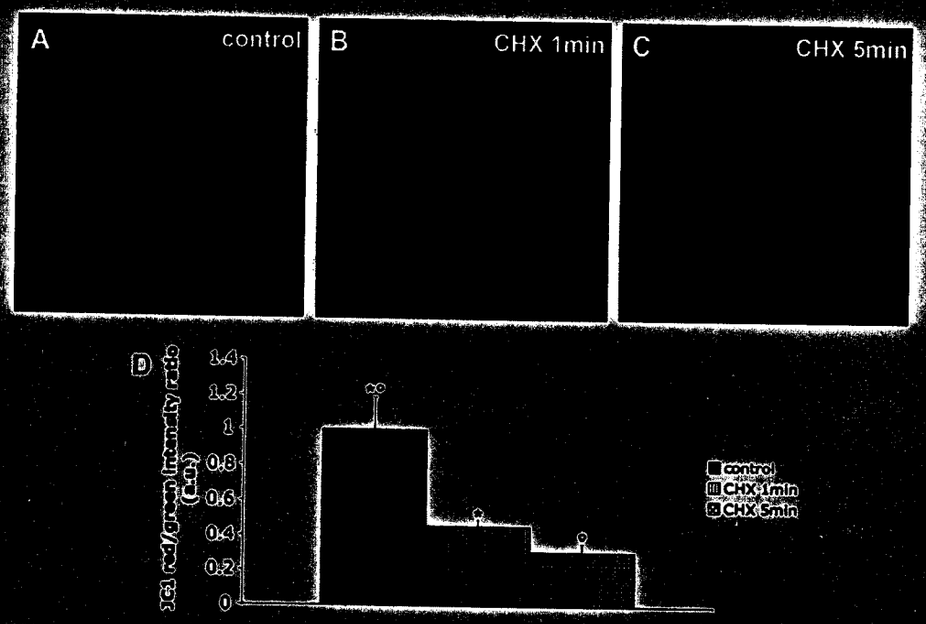

Fig. 4. Effects of CHX on mitochondrial function. (A–C) Confocal analysis of JC-1 dye staining in Saos-2 cells (300×). The treatment with CHX 0.01% for 1 min causes a shift from red (A) to green fluorescence in some of the mitochondria indicating a reduction in mitochondrial membrane potential (B). Prolongation of the exposure time caused a remarkable increase in the green fluorescence (C). (D) Quantitative analysis of red/green fluorescent intensity ratio in the indicated experimental conditions ($^{*}P < 0.05$, $^{**}P < 0.01$). All the images are representative of at least three independent experiments with similar results.

key step in the processes of cell apoptosis and necrosis (Li et al., 2007; Brown, 2007). Indeed, in the control groups, the red/green ratio was significantly higher than in the treated ones ($^{**}P < 0.01$, $^{*}P < 0.05$). Longer exposure times essentially caused a more remarkable shift from red to green fluorescence (Fig. 4C) and the red/green ratio reached the lowest level (Fig. 4D). The ability of CHX to perturb mitochondrial membrane potential was also tested in the other cell types examined and the results obtained were comparable to those found in the osteoblasts (data not shown).

3.4. Intracellular Ca^{2+} increase and reactive oxygen species (ROS) generation in osteoblasts exposed to chlorhexidine

To evaluate the possible signaling pathways underlying CHX-induced cell death, we next investigated the ability of this compound to induce intracellular Ca^{2+} accumulation and provoke ROS generation in Saos-2 osteoblastic cells. To reveal Ca^{2+} increase, living cells were visualized in time course by confocal microscopy using Fluo-3 AM as an indicator. It was found that the addition of CHX (0.01%) to the cell media elicited a rapid elevation (within 50 s) in the cytoplasmic and nuclear Ca^{2+} concentration (Fig. 5 row A), whereas the addition of PBS to the cell culture was ineffective (Fig. 5 row B). Intracellular ROS generation was analyzed using the fluorogenic substrate CM-H_2 DCFDA. Significant generation of ROS started after 30 min from treatment with CHX (Fig. 5 row C). By that time, in fact, there was a remarkable increase in 2′,7′-dichlorofluorescein (DCF) fluorescence, indicative the ROS-dependent generation of DCF in the treated cells compared with vehicle-treated control cells (Fig. 5 row D). ROS generation remained elevated throughout the observation period (additional 30 min).

4. Discussion

It is well documented that CHX has a bacteriostatic effect when used at low concentrations and a bactericidal effect at high concentrations (Oosterwaal et al., 1989). These actions are based on its ability to alter the integrity of the bacterial inner membrane leading to increased permeability and leakage of intracellular ions (Kuyyakamond and Quesnel, 1992). Because of its efficacy, CHX has been introduced in different concentrations and formulations in several commercial products for dental hygiene such as toothpaste, mouthwash, gels, sprays, chewing gums. However, in the last decade, evidence is increasing that CHX may have deleterious effects on cells *in vitro* (Pucher and Daniel, 1992; Cline and Layman, 1992; Mariotti and Rumpf, 1999), but the mechanisms underlying its cytotoxicity have not been described to date. In this study, experiments were designed to obtain more information on this issue using lines of cells (osteoblastic, endothelial and fibroblastic cells) which could represent common targets for the toxic substance in the surgical procedures for the treatment of periodontitis and peri-implantitis. *In vitro* cytotoxicity assay showed that CHX-induced cell damage in a concentration and time-dependent manner and was effective at concentrations far below (about 200-fold) those used in clinical practice, in all the cell types examined. Of interest, we also showed that CHX was able to: (1) cause alterations in actin cytoskeletal assembly; (2) stimulate apoptosis and autophagic/necrotic cell death; (3) alter mitochondrial membrane potential, in agreement with the reported ability of the compound to induce depletion of intracellular ATP and to affect succinate dehydrogenase activity in dermal fibroblasts (Hidalgo and Dominguez, 2001), and (4) trigger intracellular Ca^{2+} increase and cause ROS generation, thus suggesting a critical role for these mediators in the signal transduction cascades underlying the toxicity of CHX in these cells. Indeed, although a direct action of CHX on mitochondrial metabolic activity cannot be excluded in our cell systems, growing evidence are in favor for considering ROS and Ca^{2+} as the "*key*" players of the execution phases of both apoptotic and necrotic cell deaths, especially for those mediated by mitochondrial dysfunctions (Malhi et al., 2006; M'Bemba-Meka et al., 2006; Wang et al., 2006; Wu et al., 2006).

It is widely accepted that the two forms of cell death frequently represent alternate outcomes of the same cellular pathway to cell death (Formigli et al., 2004). Findings by different research groups have shown that perturbation of cytosolic Ca^{2+} may lead to mitochondrial Ca^{2+} overload which causes excessive stimulation of the tricarboxylic acid cycle and enhances electron flow into the respiratory chain with concomitant overgeneration of ROS. Moreover, Ca^{2+}/calmodulin activation of nitric oxide synthase (NOS) and the subsequent nitric oxide (NO) generation can also affect mitochondrial respiration and ATP synthesis and increase ROS generation (Kroemer et al., 1998; Crompton, 1999; Koterski et al., 2005). Oxidative stress is reported to provoke damages to biomolecules, including DNA, proteins and lipids (Du et al., 2005; Shibli et al., 2006). The impact of these events on the mode of cell deaths depends mostly on the degree of mitochondrial dysfunction, the balance between free radical and their scavengers, and the energetic availability of the cells, since necrosis is typically considered the consequence of a massive ATP depletion, whereas apoptosis represents the execution of an ATP-dependent death program (Formigli et al., 2000; Chiarugi, 2005).

Of note, we have provided the first experimental evidence that endothelial cells are sensitive to CHX and that osteoblasts represent highly susceptible cells to this compound. In fact, Saos-2 cells, contrary to fibroblasts and endothelial cells, underwent massive cell death even when exposed to the lowest concentration of CHX (0.01%) for the shortest time (1 min). The mechanisms by which CHX exerts different degree of cytotoxicity in the different cell types cannot be ascertained from this study and therefore warrant further evaluation. On the other hand, preliminary studies of our group aimed to detect difference in ROS response to CHX, have shown that osteoblasts

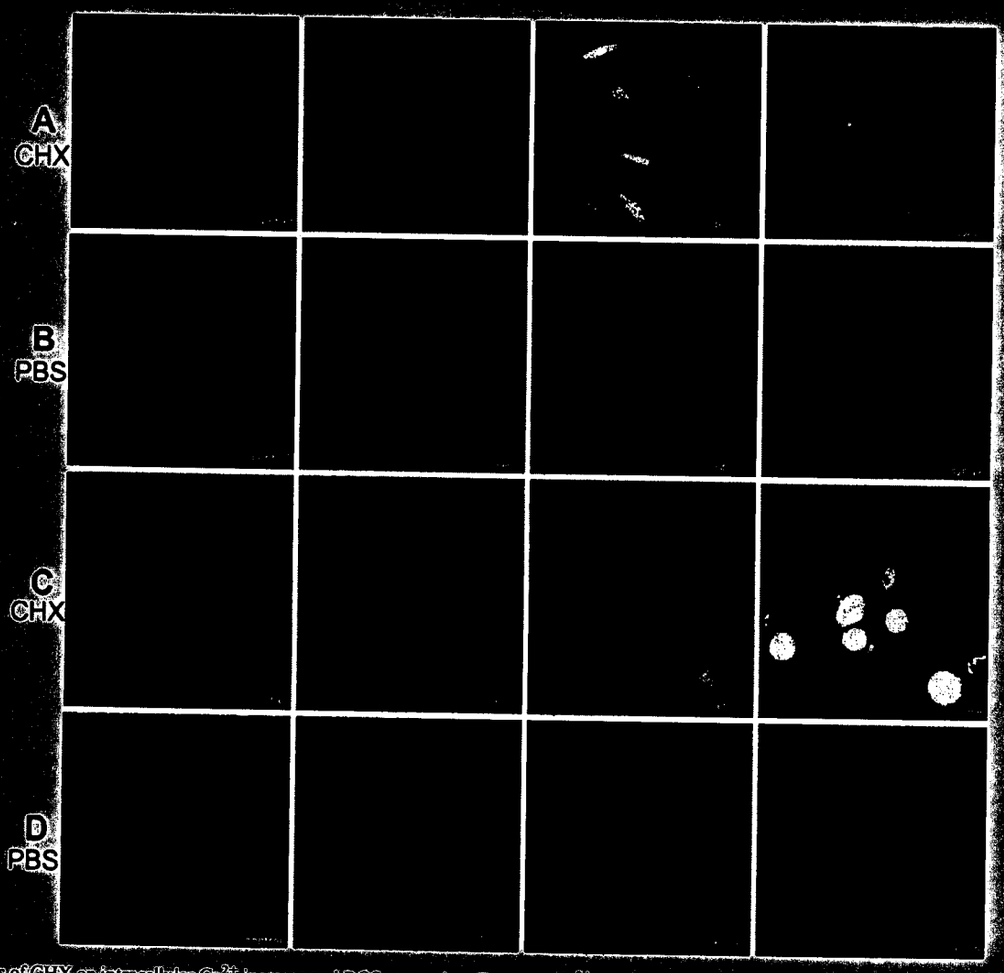

Fig. 5. Effects of CHX on intracellular Ca^{2+} increase and ROS generation. To reveal Ca^{2+} signals (rows A and B), Saos-2 cells pre-loaded with Fluo-3 AM (1 μM) were placed in open-slide flow-loading chambers, mounted on the stage of a confocal microscope and observed in Time Course. In most of the treated cells, a rapid increase in the cytoplasmic and nuclear Ca^{2+} concentration is evident soon after the application of CHX 0.01%. By contrast, the addition of PBS to the cell medium does not affect the basal fluorescence signal (250×). To reveal ROS production (rows C and D), Saos-2 cells were treated with 0.01% CHX for 1 min, loaded with 5 μM CM-H$_2$DCFDA for 20 min at 37 °C and then mounted on the stage of the confocal microscope. In some of the treated cells a remarkable increase of fluorescence intensity is visible which remain elevated throughout for the whole period of observation. By contrast the addition of PBS is unable to elicit any response (250×). All the images are representative of at least three independent experiments with similar results.

generate higher ROS levels than fibroblasts after treatment with the antimicrobic agent (Giannelli–Tani, personal communication), suggesting that the balance between ROS generation and detoxification is particularly disturbed in osteoblastic cells. These latter data may have important clinical relevance. In fact, given that osteoblasts represent the main cell type involved in bone tissue regeneration and their function is pivotal for the clinical resolution of periodontal and peri-implant intrabony defects (Shibli et al., 2006), it may be suggested that the use of CHX in periodontal and peri-implant surgery may potentially impede the healing processes of these diseases. Consistent with this, there are clinical data showing that this product delays and troubles wound healing and increases the percentage composition of granulation tissue (Bassetti and Kallenberger, 1980) when applied on mucosa-osseous wounds.

In conclusion, the results of the present study support the hypothesis that CHX is highly cytotoxic (pro-apoptotic and pro-necrotic cell death) in different cell types *in vitro* and provide evidence for the possible intracellular signaling molecules underlying the adverse effects of this compound. Hence, although the clinical significance of these findings remains to be determined, it may be suggested that the direct application of CHX during regenerative therapy for the treatment of periodontal and peri-implant diseases could have serious toxic effects on gingival fibroblasts, endothelial cells and, especially, on alveolar osteoblasts, thus negatively interfering with the early healing phase of these oral diseases. The understanding of the processes

underlying CHX-mediated effects on oral cells may be important for the development of effective strategies aimed to prevent CHX-induced cell damage and limit the adverse effects of this compound in the dental practice.

5. Conflict of interest statement

None declared.

References

Alleyn, C.D., O'Neal, R.B., Strong, S.L., Scheidt, M.J., Van Dyke, T.E., McPherson, J.C., 1991. The effect of chlorhexidine treatment of root surfaces on the attachment of human gingival fibroblast in vitro. Journal of Periodontology 62, 434–438.

Anuradha, A., Annadurai, R.S., Shashidhara, L.S., 2007. Actin cytoskeleton as a putative target of the neem limonoid Azadirachtin A. Insect Biochemistry and Molecular Biology 37, 627–634.

Babich, H., Wurzburger, B.J., Rubin, Y.L., Sinensky, M.C., Blau, L., 1995. An in vitro study on the cytotoxicity of chlorhexidine digluconate to human gingival cells. Cell Biology and Toxicology 11, 79–88.

Bassetti, C., Kallenberger, A., 1980. Influence of chlorhexidine rinsing on the healing of oral mucosa and osseous lesions. Journal of Clinical Periodontology 7, 443–456.

Becker, W., Becker, B.E., Newman, M.G., Nyman, S., 1990. Clinical and microbiologic findings that may contribute to dental implant failure. The International Journal of Oral Maxillofacial Implants 5, 31–38.

Beighton, D., Decker, J., Homer, K.A., 1991. Effects of chlorhexidine on proteolytic and glycosidic enzyme activities of dental plaque bacteria. Journal of Clinical Periodontology 18, 85–89.

Brown, G.C., 2007. Nitric oxide and mitochondria. Frontiers in Bioscience 12, 1024–1033.

Buchter, A., Kleinheinz, J., Meyer, U., Joos, U., 2004. Treatment of severe peri-implant bone loss using autogenous bone and a bioabsorbable polymer that delivered doxycycline (Atridox). British Journal of Oral Maxillofacial Surgery 42, 434–436.

Cabral, C.T., Fernandes, M.H., 2007. In vitro comparison of chlorhexidine and povidone-iodine on the long-term proliferation and functional activity of human alveolar bone cells. Clinical Oral Investigations 11, 155–164.

Cadosch, J., Zimmermann, U., Ruppert, M., Guindy, J., Case, D., Zappa, U., 2003. Root surface debridement and endotoxin removal. Journal of Periodontal Research 38, 229–236.

Chiarugi, A., 2005. "Simple but not simpler": toward a unified picture of energy requirements in cell death. The FASEB Journal 19, 1783–1788.

Cline, N.V., Layman, D.L., 1992. The effects of chlorhexidine on the attachment and growth of cultured human periodontal cells. Journal of Periodontology 63, 598–602.

Crompton, M., 1999. The mitochondrial permeability transition pore and its role in cell death. Biochemical Journal 341, 233–249.

Cronan, G.A., Potempa, J., Travis, J., Mayo, J.A., 2006. Inhibition of Porphyromonas gingivalis proteinases (gingipains) by chlorhexidine: synergistic effect of Zn(II). Oral Microbiology and Immunology 21, 212–217.

Drisko, C.H., 2001. Nonsurgical periodontal therapy. Periodontology 2000 (25), 77–88.

Drisko, C.L., Cobb, C.M., Killoy, W.J., Michalowicz, B.S., Pihlstrom, B.L., Lowenguth, R.A., Caton, J.G., Encarnacion, M., Knowles, M., Goodson, J.M., 1995. Evaluation of periodontal treatments using controlled-release tetracycline fibers: clinical response. Journal of Periodontology 66, 692–699.

Du, C., Schneider, G.B., Zaharias, R., Abbott, C., Seabold, D., Stanford, C., Moradian-Oldak, J., 2005. Apatite/amelogenin coating on titanium promotes osteogenic gene expression. Journal of Dental Research 84, 1070–1074.

Eke, P.I., Braswell, L.D., Fritz, M.E., 1998. Microbiota associated with experimental peri-implantitis and periodontitis in adult Macaca mulatta monkeys. Journal of Periodontology 69, 190–194.

Eren, K., Ozmeric, N., Sardas, S., 2002. Monitoring of buccal epithelial cells by alkaline comet assay (single cell gel-electrophoresis technique) in cytogenetic evaluation of chlorhexidine. Clinical Oral Investigations 6, 150–154.

Formigli, L., Papucci, L., Tani, A., Schiavone, N., Tempestini, A., Orlandini, G.E., Capaccioli, S., Zecchi-Orlandini, S., 2000. Aponecrosis: morphological and biochemical exploration of a syncretic process of cell death sharing apoptosis and necrosis. Journal of Cellular Physiology 182, 41–49.

Formigli, L., Conti, A., Lippi, D., 2004. "Falling leaves": a survey of the history of apoptosis. Minerva Medica 95, 159–164.

Gendron, R., Grenier, D., Sorsa, T., Mayrand, D., 1999. Inhibition of the activities of matrix metalloproteinases 2, 8, and 9 by chlorhexidine. Clinical and Diagnostic Laboratory Immunology 6, 437–439.

Gourlay, C.W., Ayscough, K.R., 2006. Actin-induced hyperactivation of the Ras signaling pathway leads to apoptosis in *Saccharomyces cerevisiae*. Molecular and Cellular Biology 26, 6487–6501.

Hidalgo, E., Dominguez, C., 2001. Mechanisms underlying chlorhexidine-induced cytotoxicity. Toxicology in vitro 15, 271–276.

Hoang, T., Jorgensen, M.G., Keim, R.G., Pattison, A.M., Slots, J., 2003. Povidone-iodine as a periodontal pocket disinfectant. Journal of Periodontal Research 38, 311–317.

Jeffcoat, M.K., Bray, K.S., Ciancio, S.G., Dentino, A.R., Fine, D.H., Gordon, J.M., Gunsolley, J.C., Killoy, W.J., Lowenguth, R.A., Magnusson, N.I., Offenbacher, S., Palcanis, K.G., Proskin, H.M., Finkelman, R.D., Flashner, M., 1998. Adjunctive use of a subgingival controlled-release chlorhexidine chip reduces probing depth and improves attachment level compared with scaling and root planing alone. Journal of Periodontology 69, 989–997.

Koterski, J.F., Nahvi, M., Venkatesan, M.M., Haimovich, B., 2005. Virulent *Shigella flexneri* causes damage to mitochondria and triggers necrosis in infected human monocyte-derived macrophages. Infection and Immunity 73, 504–513.

Kroemer, G., Dallaporta, B., Resche-Rigon, M., 1998. The mitochondrial death/life regulator in apoptosis and necrosis. Annual Review of Physiology 60, 619–642.

Kuyyakanond, T., Quesnel, L.B., 1992. The mechanism of action of chlorhexidine. FEMS Microbiology Letters 100, 211–215.

Li, J., Wang, J., Zeng, Y., 2007. Peripheral benzodiazepine receptor ligand, PK11195 induces mitochondria cytochrome c release and dissipation of mitochondria potential via induction of mitochondria permeability transition. European Journal of Pharmacology 560, 117–122.

Listgarten, M.A., Lai, C.H., 1999. Comparative microbiological characteristics of failing implants and periodontally diseased teeth. Journal of Periodontology 70, 431–437.

M'Bemba-Meka, P., Lemieux, N., Chakrabarti, S.K., 2006. Role of oxidative stress, mitochondrial membrane potential, and calcium homeostasis in nickel subsulfide-induced human lymphocyte death in vitro. Science of the Total Environment 369, 21–34.

Malhi, H., Gores, G.J., Lemasters, J.J., 2006. Apoptosis and necrosis in the liver: a tale of two deaths? Hepatology 43, S31–S44.

Mariotti, A.J., Rumpf, D.A., 1999. Chlorhexidine-induced changes to human gingival fibroblast collagen and non-collagen protein production. Journal of Periodontology 70, 1443–1448.

Mombelli, A., Lang, N.P., 1992. Antimicrobial treatment of peri-implant infections. Clinical Oral Implant Research 3, 162–168.

Mombelli, A., van Oosten, M.A.C., Schürch, E., Land, N.P., 1987. The microbiota associated with successful or failing osseointegrated titanium implants. Oral Microbiology and Immunology 2, 145–151.

Mosmann, T., 1983. Rapid colorimetric assay for cellular growth and survival: application to proliferation and cytotoxicity assays. Journal of Immunological Methods 16, 55–63.

Mustafa, K., Wroblewski, J., Hultenby, K., Silva Lopez, B., Arvidson, K., 2003. Effects of titanium surfaces blasted with TiO_2 particles on the

initial attachment of cells derived from human mandibular bone. Clinical Oral Implant Research 11, 116–128.

Oosterwaal, P.H.M., Mikx, F.H.M., van den Brink, M.E., Renggli, H.H., 1989. Bactericidal concentration of chlorhexidine-digluconate, amine-fluoride gel and stannous fluoride gel for subgingival bacteria tested in serum at short contact times. Journal of Periodontal Research 24, 155–160.

Picri, L., Bucciantini, M., Nosi, D., Formigli, L., Savistchenko, J., Melki, R., Stefani, M., 2006. The yeast prion Ure2p native-like assemblies are toxic to mammalian cells regardless of their aggregation state. Journal of Biological Chemistry 281, 15337–15344.

Pitten, F.A., Kramer, A., 1999. Antimicrobial efficacy of antiseptic mouthrinse solutions. European Journal of Clinical Pharmacology 55, 95–100.

Pucher, J.J., Daniel, J.C., 1992. The effects of chlorhexidine digluconate on human fibroblasts in vitro. Journal of Periodontology 63, 526–532.

Quirynen, M., Bollen, C.M.L., Vandekerckhove, B.N., Dekeyser, C., Papaioannou, W., Eyssen, H., 1995. Full-vs. partial mouth disinfection in the treatment of periodontal infections: short-term clinical and microbiological observations. Journal of Dental Research 67, 1456–1467.

Rams, T.E., Slots, J., 1996. Local delivery of antimicrobial agents in the periodontal pocket. Periodontology 2000 (10), 139–159.

Renvert, S., Lessem, J., Dahlén, G., Lindahl, C., Svensson, M., 2006. Topical minocycline microspheres versus topical chlorhexidine gel as an adjunct to mechanical debridement of incipient peri-implant infections: a randomized clinical trial. Journal of Clinical Periodontology 33, 362–369.

Ribeiro, D.A., Bazo, A.P., da Silva Franchi, C.A., Marques, M.E.A., Salvatori, D.M.F., 2004. Chlorhexidine induces DNA damage in rat peripheral leukocytes and oral mucosal cells. Journal of Periodontal Research 39, 358–361.

Sbordone, L., Ramaglia, L., Gulletta, E., Iacono, V., 1990. Recolonization of the subgingival microflora after scaling and root planing in human periodontitis. Journal of Periodontology 61, 579–584.

Shibli, J.A., Martins, M.C., Nociti Jr., F.H., Garcia, V.G., Marcantonio Jr., E., 2003. Treatment of ligature-induced peri-implantitis by lethal photosensitization and guided bone regeneration: a preliminary histologic study in dogs. Journal of Periodontology 74, 338–345.

Shibli, J.A., Martins, M.C., Ribeiro, F.S., Garcia, V.G., Nociti Jr., F.H., Marcantonio Jr., E., 2006. Lethal photosensitization and guided bone regeneration in treatment of peri-implantitis: an experimental study in dogs. Clinical Oral Implant Research 17, 278–281.

Slots, J., Genco, R.J., 1984. Black-pigmented Bacteroides species, Capnocytophaga species, and Actinobacillus actinomycetemcomitans in human periodontal disease: virulence factors in colonization, survival, and tissue destruction. Journal of Dental Research 63, 412–421.

Slots, J., Rams, T.E., Schonfeld, S.E., 1991. In vitro activity of chlorhexidine against enteric rods, pseudomonads and acinetobacter from human periodontitis. Oral Microbiology and Immunology 6, 62–64.

Stelzel, M., Flores-de-Jacoby, L., 1996. Topical metronidazole application compared with subgingival scaling. A clinical and microbiological study on recall patients. Journal of Clinical Periodontology 23, 24–29.

Vianna, M.E., Gomes, B.P., Berber, V.B., Zaia, A.A., Ferraz, C.C.R., de Souza-Filho, F.J., 2004. In vitro evaluation of the antimicrobial activity of chlorhexidine and sodium hypochlorite. Oral Surgery, Oral Medicine, Oral Pathology, Oral Radiology and Endodontics 97, 79–84.

Wang, X.S., Yang, W., Tao, S.J., Li, K., Li, M., Dong, J.H., Wang, M.W., 2006. The effect of δ-elemene on hela cell lines by apoptosis induction. Yakugaku Zasshi 126, 979–990.

Wardman, P., 2007. Fluorescent and luminescent probes for measurement of oxidative and nitrosative species in cells and tissues: Progress, pitfalls, and prospects. Free Radical Biology and Medicine 43, 995–1022.

Wu, C.C., Lin, J.P., Yang, J.S., Chou, S.T., Chen, S.C., Lin, Y.T., Lin, H.L., Chung, J.G., 2006. Capsaicin induced cell cycle arrest and apoptosis in human esophagus epidermoid carcinoma CE 81T/VGH cells through the elevation of intracellular reactive oxygen species and Ca^{2+} productions and caspase-3 activation. Mutation Research 601, 71–82.